

Supporting Information for

Synthesis, Crystal Structure and Optical Properties of the First Alkali Metal Rare Earth Iodate Fluoride: Li₂Ce(IO₃)₄F₂

Changcheng Tang,^{a,b} Xingxing Jiang,^a Shu Guo,^{a,d†} Ruixin Guo,^{a,b} Lijuan Liu,^a Mingjun Xia,^a Qian Huang,^c Zheshuai Lin,^{a,b} Xiaoyang Wang*^a

a. Beijing Center for Crystal Research and Development, Key Laboratory of Functional Crystals and Laser Technology of Chinese Academy of Sciences, Technical Institute of Physics and Chemistry, Chinese Academy of Sciences, Beijing 100190, China.

b. University of Chinese Academy of Sciences, Beijing 100049, China

c. Institute of Engineering Thermophysics, Chinese Academy of Sciences, Beijing 100190, China.

d. †Present address: Department of Chemistry, Princeton University, Princeton, NJ 08544, USA

Content

1. Experimental section and First principle calculation

2. Tables and figures

Table S1. Crystallographic record and structural refinement information

Table S2. Fractional atomic coordinates and isotropic or equivalent isotropic displacement parameters (\AA^2)

Table S3. Atomic displacement parameters ($\text{\AA}^2 \times 10^2$)

Table S4. Selected geometric information (\AA , $^\circ$)

Table S5. Elements analysis by Energy dispersive X-ray spectroscopy (EDX) of $\text{Li}_2\text{Ce}(\text{IO}_3)_4\text{F}_2$

Table S6. The calculated refractive indices n and the birefringence Δn of $\text{Li}_2\text{Ce}(\text{IO}_3)_4\text{F}_2$ crystal

Figure S1. As-grown crystals of $\text{Li}_2\text{Ce}(\text{IO}_3)_4\text{F}_2$.

Figure S2. Calculated(red) and experimental(blue) XRD patterns of $\text{Li}_2\text{Ce}(\text{IO}_3)_4\text{F}_2$

Figure S3. Comparison of the powder XRD patterns of the thermal experimental residue (heating to 400°C) and CeO_2 / LiF standards

3. References

1. Experimental section and First principle calculation

The purity of all ingredient was confirmed by powder X-ray diffraction.

Synthesis. LiF(\geq 99.8%) is purchased from Macklin, HIO₄.2(H₂O)(AR) and HIO₃(AR, 99.5%) are purchased from Aladdin Industrial Corporation, Ce(NO₃)₃.6H₂O (\geq 99%) is purchased from Xilong Scientific Co., Ltd. We have grown the Li₂Ce(IO₃)₄F₂ crystals by hydrothermal method with the mixture of LiF/ HIO₄.2(H₂O)/ HIO₃/ Ce(NO₃)₃.6H₂O at a molar concentration ratio of 3~5:1~2:3~5:1. The mixture was heated at 520 K for 5 days, then cooled to 480 K at a rate of 0.5 Kh⁻¹ and cooled to 303 K at a rate of 2 Kh⁻¹. The product was washed by deionized water and the millimeter-sized single crystals of Li₂Ce(IO₃)₄F₂ in almost 100% yield (based on Ce) were obtained (**Figure S1**).

Single crystal X-ray diffraction. A yellow block crystal was selected for single crystal XRD data collection which is carried on a Bruker APEX II single crystal X-ray diffractometer by using a graphite-monochromator Mo K α radiation ($\lambda = 0.71073\text{\AA}$) and Bruker APEX-II CCD equipment at 153 K. The diffraction intensity data, cell refinements and diffraction data reduction are carried out by the CrystalClear program. The structure was worked out by direct methods and refined by the full matrix least squares on F² by SHELXL-97.¹ The Crystallographic record and structural refinement information are listed in **Table S1**. The fractional atomic coordinates and isotropic or equivalent isotropic displacement parameters, atomic displacement parameters, selected geometric parameters were listed in **Table S2-4**. The CCDC number of this crystal is 1874673.

Powder X-ray diffraction. The powder XRD was carried on an automated Bruker D8 ADVANCE X-ray diffractometer by using Cu K α radiation ($\lambda = 1.5418 \text{\AA}$) at indoor temperature , the 2 θ range from 5° to 80° with a 0.2s / step time and a 0.02° scan step width.. (**Figure S2**)

Infrared (IR) spectroscopy. 3 mg Li₂Ce(IO₃)₄F₂ crystal powder was ground with 300 mg dried KBr powder, the mixed powder was pressed into a thin wafer under 10 MPa pressure. It was carried on an Excalibur 3100 Fourier transform infrared spectrometer at indoor temperature. The IR spectrum is recorded in the range from 400 to 4000 cm⁻¹ with a resolution of 4 cm⁻¹.

UV-vis-IR diffuse reflectance spectroscopy. 800 mg Li₂Ce(IO₃)₄F₂ crystal powder was carried on a Cary 7000 UV-vis-NIR spectrophotometer with wavelength range in 200-2500 nm and a resolution of 1 nm. The spectrum can be converted to other forms by using the Kubeka Munk function,² F(R) = (1-R)²/2R = K/S = AC/S, where R,K,S,A and C stand for the reflectance, absorption coefficients, scattering coefficient, absorbance and concentration of the absorbing species, respectively.

Elemental analysis. A number of Li₂Ce(IO₃)₄F₂ crystals were chose for elements analysis on a HITACHI S-4300 SEM with Energy Dispersive X-ray Detector (EDX). The results gave that the molar ratio of elements Ce:I:O:F is 1:4.25:18.36:2.99 (**Table S5**), which is close to the theoretical ratio 1:4:12:2. The elements analysis picture is in Figure S1.

Thermal analysis. The thermal property of Li₂Ce(IO₃)₄F₂ crystals are tested on a

NETZSCH STA 409C/CD thermal analyzer with the differential scanning calorimetric (DSC, calibrated with Al_2O_3) and thermal gravimetric (TG) Analyses. 13.24 mg $\text{Li}_2\text{Ce}(\text{IO}_3)_4\text{F}_2$ crystals are placed in a platinum crucible and followed the heating procedure: heated from 23.41°C to 1164.38°C and then cooled down to 87.86 °C at a same rate of 5 °C /min in nitrogen atmosphere.

First-principle calculation. The first-principle electronic structure calculations of $\text{Li}_2\text{Ce}(\text{IO}_3)_4\text{F}_2$ was carried out by plane-wave pseudopotential method³ implemented by CASTEP package⁴ based on density function theory⁵. The functionals developed by Perdew-Burke-Ernzerhof (PBE)⁶ in generalized gradient approximation (GGA) form was adopted to describe the exchange-correlation terms in the Hamiltonian. The effective interactions between atom cores and valence electrons ($\text{Li}1s^22s^1$, $\text{Ce}4f^15s^25p^65d^16s^2$, $\text{I}5s^25p^5$, $\text{O}2s^22p^4$ and $\text{F}2s^22p^5$) are modeled by the optimized normal-conserving pseudopotentials(NCP)⁷. To achieve energy convergence, the kinetic energy cutoff is 940 eV and Monkhorst-Pack⁸ k-point meshes in Brillouin zone is set as $3\times3\times1/\text{\AA}^{-3}$. Because of the discontinuity of exchange-correlation energy used by PBE functionals in standard DFT framework, the calculated band gap is smaller than experimental value. A scissor operator is chosen to correct the GGA method bandgap value. Based on the scissor-corrected band structure, the imaginary part of the dielectric function is calculated by the electron transition across the band gap, and the real part, i.e., refractive index could be obtained by Kramers-Kronig relations⁹:

$$\varepsilon_1(\omega) = \frac{P}{\pi} \int_{-\infty}^{\infty} \frac{\varepsilon_2(\omega')}{\omega' - \omega} d\omega'$$

Based on the calculated refractive index (n_x , n_y , n_z), birefringence ($\Delta n = n_z - n_y$) could be obtained.

2. Tables and figures

Table S1. Crystallographic record and structural refinement information

Empirical formula	Li ₂ CeI ₄ O ₁₂ F ₂
Formula weight(g/mol)	891.60
Temperature(K)	153
Wavelength (Å)	0.71073
Crystal system	<i>Monoclinic</i>
Space group	<i>C2/c</i>
<i>a</i> (Å)	12.5663(6)
<i>b</i> (Å)	5.5853(3)
<i>c</i> (Å)	17.1623(8)
$\beta(^{\circ})$	95.953 (4)
Volume(Å ³)	1198.07(1)
Z	4
Density (g cm ⁻³)	4.943
μ (mm ⁻¹)	14.20
<i>F</i> (000)	1560
R1,wR2 [$I > 2\sigma(I)$] ^a	0.0136, 0.0307
R1,wR2[all data] ^a	0.0144, 0.0310
^a $R_1 = \sum F_o - F_c / \sum F_o $; $wR_2 = \{(\sum [w(F_o^2 - F_c^2)^2] / \sum wF_o^4\}^{1/2}$	

Table S2. Fractional atomic coordinates and isotropic or equivalent isotropic

Atom	Wyck.	x/a	y/b	z/c	$U_{\text{iso}}^*/U_{\text{eq}}$	BVS
Li1	8f	0.3812(6)	-0.0074(1)	0.4333(4)	0.0233(2)	0.91
Ce1	4e	0.5	0.07750(5)	0.25	0.00753(9)	3.68
I1	8f	0.604706(2)	0.46888(4)	0.429972(1)	0.00900(8)	5.08
I2	8f	0.784840(2)	-0.03115(4)	0.336792(1)	0.00797(8)	4.95
F1	8f	0.43997(2)	-0.1265(4)	0.34393(1)	0.0147(4)	-0.86
O2	8f	0.5247(2)	0.3809(4)	0.33947(1)	0.0151(5)	-2.09
O3	8f	0.64418(2)	-0.1141(4)	0.32693(1)	0.0136(5)	-2.02
O4	8f	0.8205(2)	-0.1755(5)	0.42970(1)	0.0156(6)	-1.94
O5	8f	0.82524(2)	-0.2631(5)	0.27105(2)	0.0146(5)	-1.94
O6	8f	0.5521(2)	0.2499(5)	0.49212(2)	0.0170(6)	-1.99
O7	8f	0.73098(2)	0.3369(5)	0.41412(2)	0.0164(6)	-1.93

Table S3. Atomic displacement parameters (\AA^2)

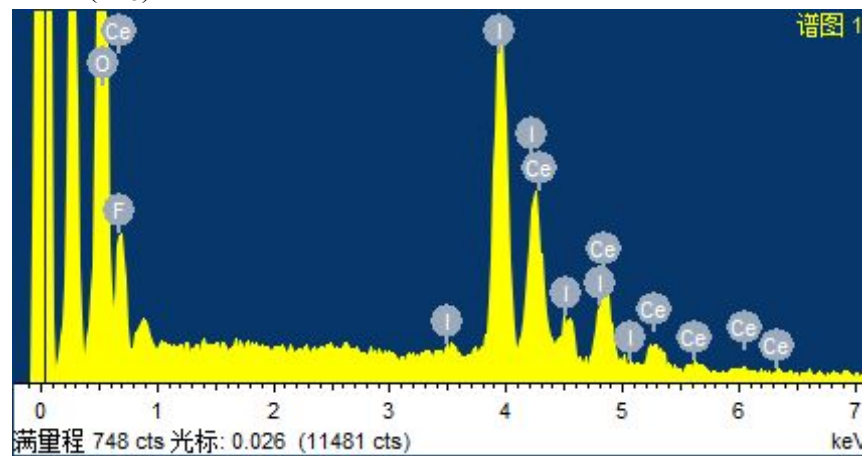
atoms	U^{11}	U^{22}	U^{33}	U^{12}	U^{13}	U^{23}
Ce1	0.00633(1)	0.00885(2)	0.00742(1)	0	0.00075(1)	0
I1	0.00947(1)	0.00990(1)	0.00764(1)	-0.00008(8)	0.00099(9)	-0.00052(8)
I2	0.00665(1)	0.00859(1)	0.00859(1)	0.00034(8)	0.00048(8)	-0.00062(8)
F1	0.0146(1)	0.0161(1)	0.0140(1)	0.0004(8)	0.0037(8)	0.0023(9)
O2	0.0176(1)	0.0128(1)	0.0138(1)	0.0001(1)	-0.0040(1)	-0.0028(1)
O3	0.0090(1)	0.0152(1)	0.0162(1)	-0.0021(1)	-0.0005(1)	0.0048(1)
O4	0.0196(1)	0.0170(1)	0.0093(1)	0.0061(1)	-0.0022(1)	-0.0005(1)
O5	0.0101(1)	0.0174(1)	0.0162(1)	0.0036(1)	0.0015 (1)	-0.0067(1)
O6	0.0147(1)	0.0185(1)	0.0186(1)	-0.0006(1)	0.0048 (1)	0.0087(1)
O7	0.0100(1)	0.0183(1)	0.0211(1)	0.0023(1)	0.0030 (1)	-0.0055(1)
Li1	0.033(4)	0.023(4)	0.016(3)	0.010(3)	0.007 (3)	0.003 (3)

Table S4. Selected geometric information (\AA , $^\circ$)

Ce1—F1 ⁱ	2.172 (2)	I2—O4	1.801 (2)
Ce1—F1	2.172 (2)	I2—O3	1.818 (2)
Ce1—O2	2.286 (2)	I2—O5	1.824 (2)
Ce1—O2 ⁱ	2.286 (2)	F1—Li1	1.892 (7)
Ce1—O3 ⁱ	2.382 (2)	O4—Li1 ^{iv}	2.003 (7)
Ce1—O3	2.382 (2)	O5—Ce1 ^{iv}	2.431 (2)
Ce1—O5 ⁱⁱ	2.431 (2)	O6—Li1 ^v	1.988 (7)
Ce1—O5 ⁱⁱⁱ	2.431 (2)	O7—Li1 ^{vi}	2.073 (8)
I1—O6	1.794 (2)	Li1—O6 ^v	1.988 (7)
I1—O7	1.796 (2)	Li1—O4 ⁱⁱ	2.003 (7)
I1—O2	1.828 (2)	Li1—O7 ^{vii}	2.073 (8)
F1 ⁱ —Ce1—F1	116.72 (1)	O2—Ce1—O5 ⁱⁱ	71.98 (8)
F1 ⁱ —Ce1—O2	148.63 (9)	O2 ⁱ —Ce1—O5 ⁱⁱ	76.49 (9)
F1—Ce1—O2	85.63 (8)	O3 ⁱ —Ce1—O5 ⁱⁱ	66.43 (8)
F1 ⁱ —Ce1—O2 ⁱ	85.63 (8)	O3—Ce1—O5 ⁱⁱ	136.80 (8)
F1—Ce1—O2 ⁱ	148.63 (9)	F1 ⁱ —Ce1—O5 ⁱⁱⁱ	72.14 (8)
O2—Ce1—O2 ⁱ	84.34 (1)	F1—Ce1—O5 ⁱⁱⁱ	133.71 (8)
F1 ⁱ —Ce1—O3 ⁱ	69.86 (8)	O2—Ce1—O5 ⁱⁱⁱ	76.49 (9)
F1—Ce1—O3 ⁱ	82.70 (8)	O2 ⁱ —Ce1—O5 ⁱⁱⁱ	71.98 (8)
O2—Ce1—O3 ⁱ	138.40 (9)	O3 ⁱ —Ce1—O5 ⁱⁱⁱ	136.80 (8)
O2 ⁱ —Ce1—O3 ⁱ	85.31 (9)	O3—Ce1—O5 ⁱⁱⁱ	66.43 (8)
F1 ⁱ —Ce1—O3	82.70 (8)	O5 ⁱⁱ —Ce1—O5 ⁱⁱⁱ	137.03 (1)
F1—Ce1—O3	69.86 (8)	O6—I1—O7	101.33 (1)
O2—Ce1—O3	85.31 (9)	O6—I1—O2	96.75 (1)
O2 ⁱ —Ce1—O3	138.40 (9)	O7—I1—O2	100.23 (1)
O3 ⁱ —Ce1—O3	126.60 (1)	O4—I2—O3	96.82 (1)
F1 ⁱ —Ce1—O5 ⁱⁱ	133.71 (8)	O4—I2—O5	99.78 (1)
F1—Ce1—O5 ⁱⁱ	72.14 (8)	O3—I2—O5	95.26 (1)

Symmetry codes: (i) $-x+1, y, -z+1/2$; (ii) $x-1/2, y+1/2, z$; (iii) $-x+3/2, y+1/2, -z+1/2$; (iv) $x+1/2, y-1/2, z$; (v) $-x+1, -y, -z+1$; (vi) $x+1/2, y+1/2, z$; (vii) $x-1/2, y-1/2, z$.

Table S5. Elements analysis by Energy dispersive X-ray spectroscopy (EDX) of $\text{Li}_2\text{Ce}(\text{IO}_3)_4\text{F}_2$



Element	Mass (%)	Molar (%)
O K	28.51	69.02
F K	5.51	11.23
I L	52.38	15.99
Ce L	13.60	3.76
Total	100.00	100.00

Table S6. The calculated refractive indices n and the birefringence Δn of $\text{Li}_2\text{Ce}(\text{IO}_3)_4\text{F}_2$ crystal

Wavelength(nm)	n_x	n_y	n_z	Δn
2479.555	1.89629	1.89628	1.95158	0.0553
2236.073	1.89745	1.89744	1.95277	0.05533
2036.133	1.89874	1.89873	1.9541	0.05537
1869.011	1.90016	1.90015	1.95556	0.05541
1664.13	1.90254	1.90253	1.958	0.05547
1451.919	1.9062	1.90619	1.96175	0.05556
1252.3	1.91161	1.91161	1.96728	0.05567
1074.951	1.91946	1.91945	1.97525	0.0558
886.6102	1.93443	1.93443	1.99034	0.05591
696.7212	1.96817	1.96818	2.02365	0.05547
588.6568	2.01217	2.01218	2.06635	0.05417
533.4923	2.05111	2.05113	2.10458	0.05345
487.781	2.09571	2.09575	2.15016	0.05441
449.285	2.13952	2.13956	2.19852	0.05896

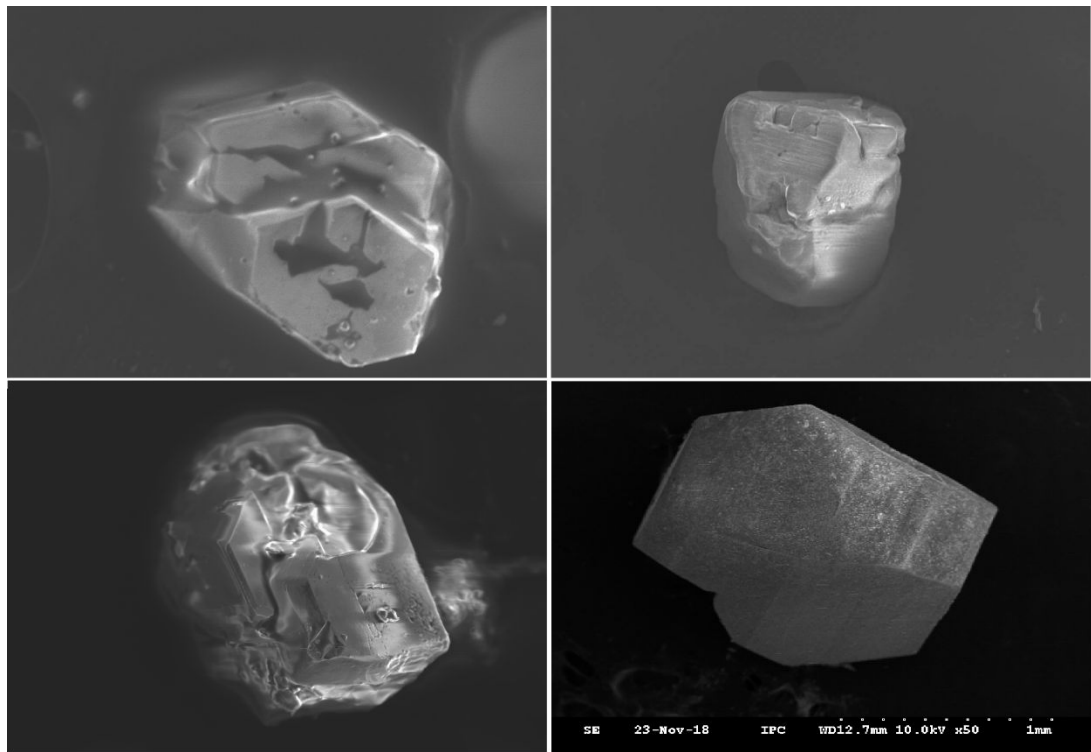


Figure S1. As-grown crystals of $\text{Li}_2\text{Ce}(\text{IO}_3)_4\text{F}_2$.

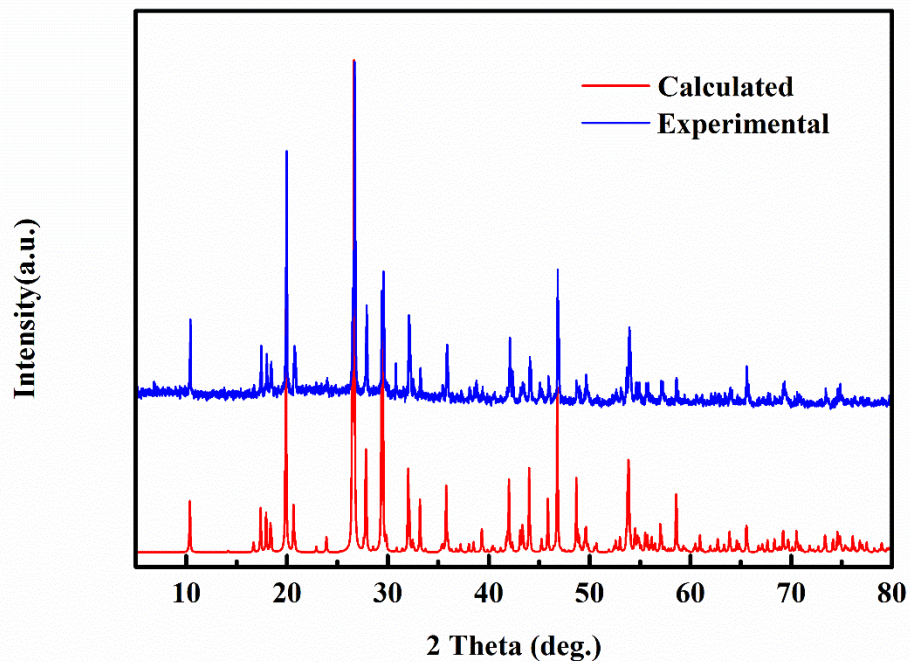


Figure S2. Calculated (red) and experimental (blue) XRD patterns of $\text{Li}_2\text{Ce}(\text{IO}_3)_4\text{F}_2$

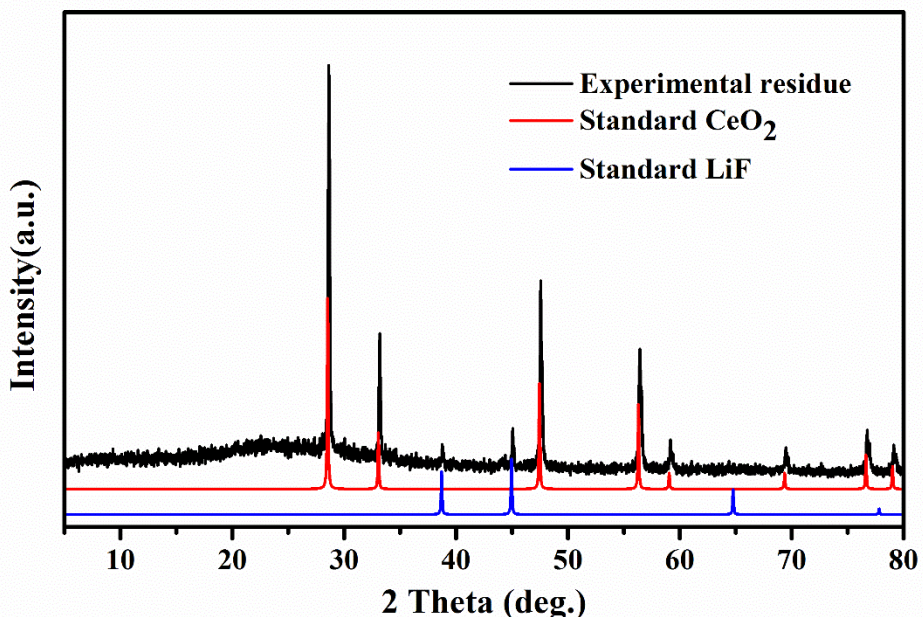


Figure S3. Comparison of the powder XRD patterns of the thermal experimental residue (heating to 400°C) and CeO₂ / LiF standards

3. References

- 1 Sheldrick, G. SHELXS97, Progr. Solut. Cryst. Struct. Univ. Göttingen Göttingen, Ger. (1997).
- 2 Schevciw, O.; White, W. B. The Optical Absorption Edge of Rare Earth Sesquisulfides and Alkaline Earth- Rare Earth Sulfides. *Mater. Res. Bull.*, **1983**, 18, 1059–1068.
- 3 Payne,M. C.; Teter, M. P. ;Allan,D. C. ;Arias, T. A. ;Joannopoulos, J. D. Iterative Minimization Techniques for ab Initio Total-energy Calculations: Molecular Dynamics and Conjugate Gradients. *Rev. Mod. Phys.*, **1992**, 64, 1045–1097.
- 4 Clark, S. J.; Segall, M. D.; Pickard, C. J.; Hasnip, P. J.; Probert, M. I. J.; Refson, K.; Payne, M. C. First Principles Methods Using CASTEP. *Z. Kristallogr.*, **2005**, 220, 567–570.
- 5 Kohn, W.; Sham, L. J. Self-Consistent Equations Including Exchange and Correlation Effects. *Phys. Rev.*, **1965**, 140, 1133–1138.
- 6 Perdew, J. P.; Wang, Y. Perdew-Wang '92 Local Spin Density Approximation, *Phys. Rev. B*, **1992**, 45, 13244–13249.
- 7 Rappe, A. M.; Rabe, K. M.; Kaxiras, E.; Joannopoulos, J. D. Optimized Pseudopotentials, *Phys. Rev. B*, **1990**, 41, 1227–1230.
- 8 Monkhorst, H. J.; Pack, J. D. "Special Points for Brillouin-Zone Integrations"—A Reply, *Phys. Rev. B*, **1977**, 16, 1748–1749.
- 9 Palik, E. D.; Prucha, E. J. Handbook of Optical Constants of Solids, *Academic Press*, **1985**.